INSTITUTE OF PHYSICS PUBLISHING SMART MATERIALS AND STRUCTURES
Smart Mater. Struct. **11** (2002) 848–853 PII: S0964-1726(02)39937-3

Strain monitoring of a filament wound composite tank using fiber Bragg grating sensors

Hyun-Kyu Kang, Jae-Sung Park, Dong-Hoon Kang, Cheol-Ung Kim, Chang-Sun Hong and Chun-Gon Kim[1]

Division of Aerospace Engineering, Korea Advanced Institute of Science and Technology, 373-1 Kusong-dong, Yusong-gu, Taejon 305-701, Korea

E-mail: cgkim@kaist.ac.kr

Received 20 August 2001, in final form 19 June 2002
Published 2 October 2002
Online at stacks.iop.org/SMS/11/848

Abstract
In this paper, we present strain monitoring of a filament wound composite tank using fiber Bragg grating (FBG) sensors during hydrostatic pressurization. 20 FBG sensors and 20 strain gages were attached to the domes and cylinder of the composite tank. A wavelength-swept fiber laser was used as a light source to supply high signal power. From the experimental results, it was successfully demonstrated that the FBG sensor system is useful for large structures that require a large number of sensor arrays.

(Some figures in this article are in colour only in the electronic version)

1. Introduction

Composite materials are increasingly being used as engineering materials in aircraft, buildings, containers, and other structures. In particular, the use of filament wound composite tanks is increasingly prevalent because of the higher specific strength and specific stiffness compared with their metal counterparts, as well as excellent corrosion and fatigue resistance. Filament wound composite tanks are finding use in applications such as fuel tanks, pressure tanks, and motor cases of aerospace structures.

The complexity in damage mechanisms and failure modes makes the use of composite materials difficult. Sometimes, the impact-induced damage is not detectable by visual inspection. Therefore, non-destructive techniques are needed to monitor the health of composite structures. Most of the conventional damage assessment and non-destructive inspection methods are time-consuming and are often difficult to implement on hard-to-reach parts of the structure. For these reasons, a built-in assessment system must be developed to constantly monitor the structural integrity of critical components. Measuring structural response in the form of strains and deflections is of great interest in the health monitoring of a structure.

Fiber optic sensors (FOS) have shown a potential to provide real-time health monitoring of the structures. They can easily be embedded in or attached to the structures and are not affected by the electromagnetic field. Also, they present not only flexibility in the selection of the sensor size but also high sensitivity. These advantages of FOS make them a potential solution for sensor systems for smart structures.

Recently, FOS have been introduced into composite structures [1–4]. The strain measurement of composite structures is of great interest in terms of the structural integrity of aerospace structures. Fiber Bragg grating (FBG) sensors based on wavelength-division multiplexing (WDM) technology are attracting considerable research interest and appear to be ideally suitable for structural health monitoring of smart composite structures. FBG sensors are easily multiplexed and have many advantages such as linear response and absolute measurement. As the spectral response of the FBG sensor signal renders the measurement free from intensity fluctuations, it guarantees reproducible measurements despite optical losses due to bending or connectors.

In this paper, the strains of a filament wound composite tank were monitored using a FBG sensor system in real time. 20 FBG sensors and 20 strain gages were attached to the surface of the dome and cylinder part of the composite tank. The strains measured by the FBG sensors were compared with those measured by strain gages.

[1] Author to whom any correspondence should be addressed.

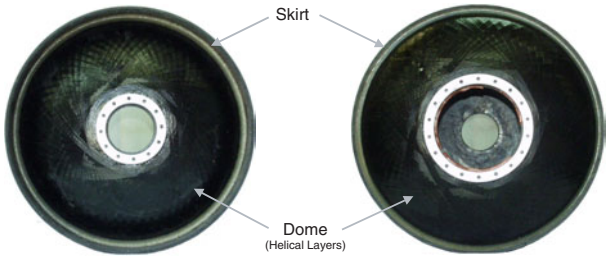

(a) Front dome. (b) Aft dome.

(c) Side view. (d) Assembly with nozzle.

Figure 1. A filament wound composite tank.

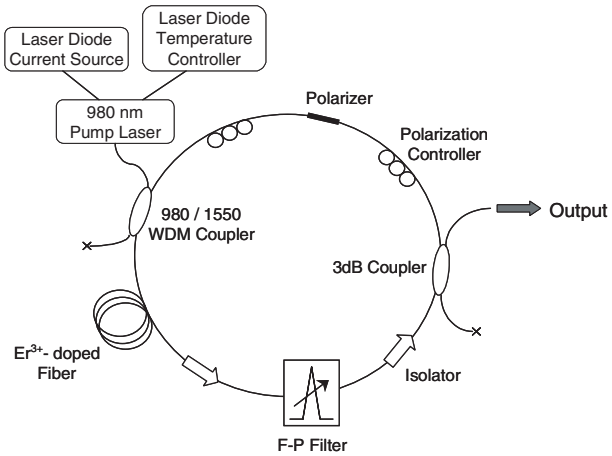

Figure 2. A schematic diagram of the WSFL.

Table 1. Dimensions of the filament wound composite tank.

	Forward dome	Aft dome
Cylinder radius, R_c	250 mm	
Boss radius, R_b	50 mm	85 mm
Cylinder thickness, t_c	2.92 mm	
Thickness of 1st skirt	4.16 mm	
Thickness of 2nd skirt	3.68 mm	

2. Fiber Bragg grating sensors

The operation of a FBG is based on a periodic, refractive index change that is produced in the core of an optical fiber by exposure to an intense UV interference pattern. This grating structure results in the reflection of the light at a specific narrow-band wavelength, called the Bragg wavelength. The Bragg condition is given by $\lambda_B = 2n_e\Lambda$, where λ_B is the Bragg wavelength of the FBG, n_e is the effective index of the fiber core, and Λ is the grating period. The shift of the Bragg wavelength due to strain and temperature can be expressed as

$$\Delta\lambda_B = \lambda_B[(\alpha_f + \xi_f)\Delta T + (1 - p_e)\varepsilon] \quad (1)$$

where α_f is the coefficient of thermal expansion (CTE), ξ_f is the thermo-optical coefficient, and p_e is the strain-optical coefficient of the optical fiber. The value of $p_e = 0.227$ was measured experimentally and used for this study. If there is no temperature change, we can measure the strain from the wavelength shift as

$$\varepsilon = \frac{1}{1 - p_e}\frac{\Delta\lambda_B}{\lambda_B}. \quad (2)$$

In this experiment, we used a dummy FBG, which was not attached to the composite tank, for the temperature compensation.

3. Experimental details

3.1. Filament wound composite tank

Figure 1 shows the filament wound composite tank, which is to be used as the third-stage kick motor case of a three-stage Korean scientific rocket (KSR). This composite tank consists of a front dome, an aft dome, a cylinder, and a skirt for joining with a satellite. Epoxy filler filled the gap between the skirt and domes to prevent stress concentration due to sudden changes of curvature and thickness in the joint part of the cylinder and domes. The composite tank was fabricated by a dry winding process using tow prepreg. The tow prepreg is a composite prepreg tape with wide bandwidth of several mm. The dome parts consist of 12 layers (helical winding layers) with $\pm 22°$ winding angle and the cylinder parts are made of helical layers and several hoop layers (90°). The helical winding layer is 0.198 mm thick per two layers ($+22°/-22°$) and the hoop winding layer is 0.168 mm thick per single layer. The first skirt and second skirt have $[\pm 30^\circ_4/90^\circ_2/\pm 30^\circ_4/90^\circ_2]$ and $[90^\circ_2/\pm 15^\circ_2/90^\circ_2/\pm 15^\circ_2/90^\circ_6]$ lay-ups, respectively. The dimensions of the filament wound composite tank are shown in table 1.

3.2. Wavelength-swept fiber laser

In this study, a wavelength-swept fiber laser (WSFL) [5], a broadband source, was used to interrogate the FBG sensors. Figure 2 shows a schematic diagram of the configuration of the WSFL. The WSFL was in a unidirectional ring configuration with isolators, a 3 dB output coupler, and an Er^{3+}-doped fiber (EDF) pumped by a laser diode at 980 nm. An F–P tunable filter was used as the intracavity scanning filter and had a 3 dB bandwidth of 0.27 nm and a free spectral range of 58 nm. We modulated the F–P filter with a triangular waveform to produce a wavelength sweep over 40 nm from 1525 to 1565 nm at a 200 Hz repetition rate. The output power of the WSFL was over 1000 times as large as that of the amplified spontaneous emission (ASE) of an LD-pumped EDF, which is usually used for the light source in a FBG sensor system [6]. The FBG sensor system has a good strain resolution less than 10 $\mu\varepsilon$ [7].

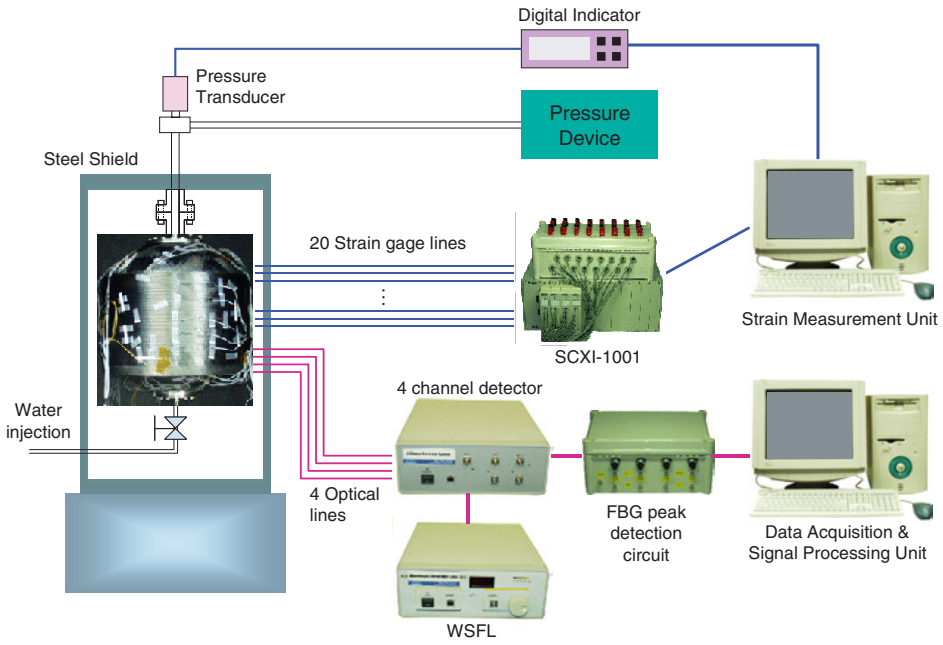

Figure 3. The experimental set-up.

3.3. Experimental apparatus and method

Figure 3 depicts the experimental set-up for the strain monitoring of a filament wound composite tank during hydrostatic pressurization. The strain measurement was performed at intervals of 100 up to 1000 psi (6.895 MPa). The data from the FBG sensors, strain gages, and a pressure transducer were acquired and processed by computers in real time. In total, 20 FBG sensors and 20 strain gages were attached at the same longitudinal locations on the composite tank. The array of FBG sensors consisted of five gratings along each of four separate fiber optic lines. Figure 4 illustrates the locations and directions of the sensors attached to the domes. The five sensors of FBG line A were attached to the front dome and the other five sensors of FBG line B on the aft dome. Figure 5 shows the locations and directions of sensors attached to the cylinder and the skirt. The five sensors of FBG line C and the five sensors of FBG line D were attached to the cylinder and the skirt. Since most of the loading applied to the composite tank is sustained by reinforcing fibers, it is important to measure the strains along the fiber direction. Hence, all sensors were aligned with fiber directions of the composite tank except two sensors of FBG line D attached to the cylinder perpendicularly to the fiber direction. On the domes, the pairs of FBG sensors and strain gages were attached to the same tow prepreg in the helical winding direction ($\pm 22^{\circ}$) of fibers and at the same longitudinal location. On the cylinder and the skirt, also, eight pairs of two sensors each were affixed in the hoop winding direction, i.e., the circumferential direction of the cylinder, and at the same longitudinal location and two pairs were affixed perpendicular to the winding direction, i.e., the longitudinal direction.

The signals of the FBG sensors, strain gages, and pressure transducer were acquired simultaneously by computers, and processed and displayed by a signal-processing program written in LabVIEW® software. The pressure level was held for checking the pressure drop that occurred due to leaking water.

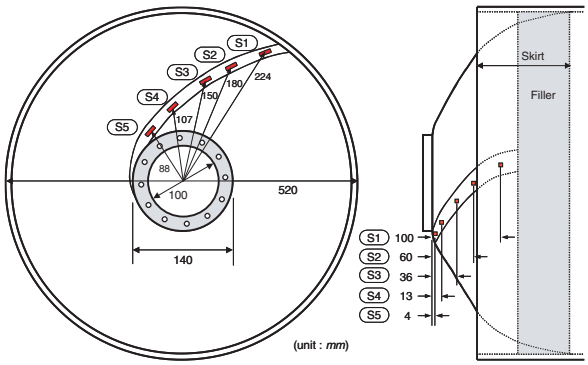

(a) Front dome – FBG line A.

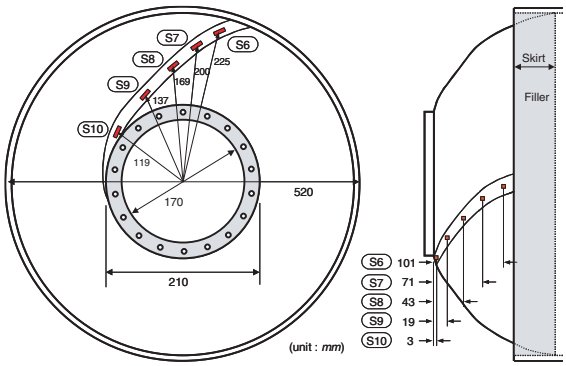

(b) Aft dome – FBG line B.

Figure 4. Locations and directions of sensors attached to the domes.

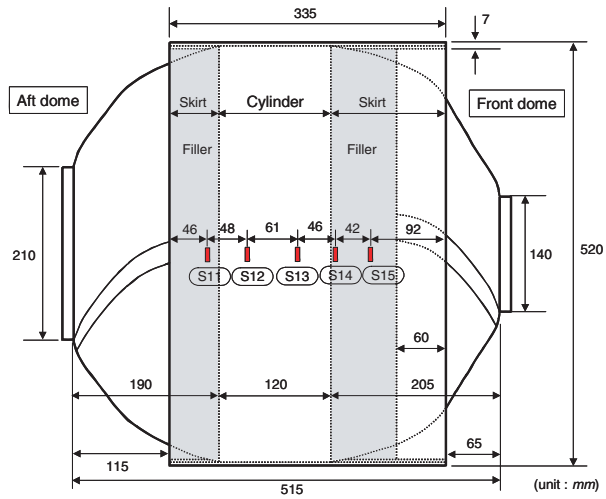

(a) Cylinder – FBG line C.

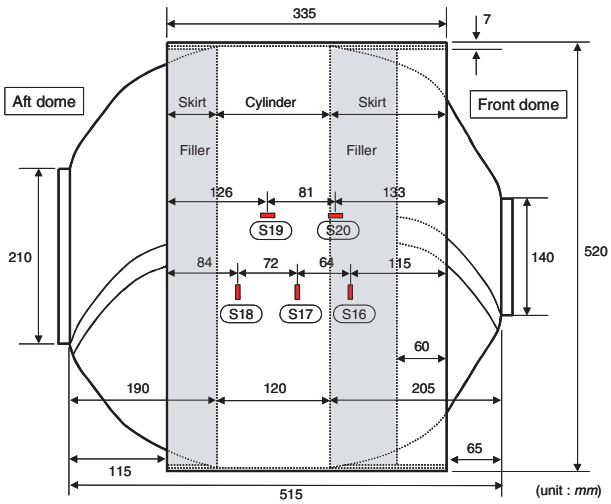

(b) Cylinder – FBG line D.

Figure 5. Locations and directions of sensors attached to the cylinder.

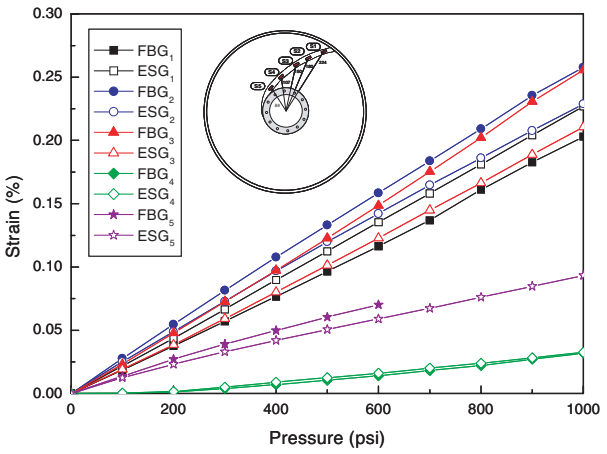

(a) Front dome – FBG line A.

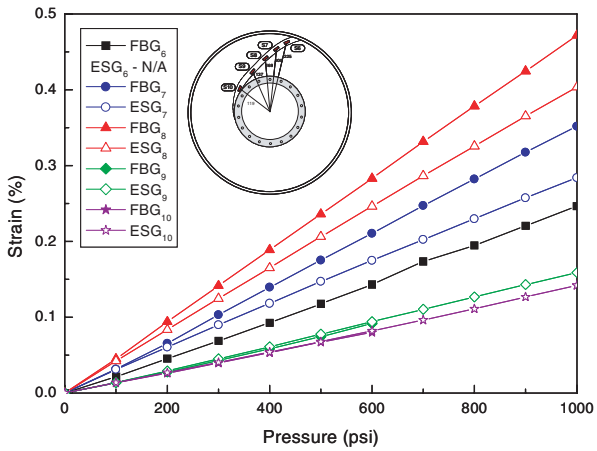

(b) Aft dome – FBG line B.

Figure 6. Strains measured by the FBG and ESG attached to the domes.

4. Results and discussion

Figures 6 and 7 illustrate results of strain measurements using the FBG sensors and electrical strain gages (ESG). As shown in these results, the strains measured by both types of sensor increased linearly with increasing pressure. The signal peaks of FBG_5 of line A, FBG_9 and FBG_{10} of line B attached to the domes split when the pressure level was over 600 psi. The signal peaks of FBG_{19} and FBG_{20} for line D attached to the cylinder split at a pressure level over 300 psi. Hence, these FBG sensors could not measure strains at those pressure levels. Also, since ESG_6 was in an abnormal condition, it could not measure the strains.

In figure 6(a), the strains measured by FBG_2 and FBG_3 were much larger than those measured by other FBG sensors on the front dome. In figure 6(b), also, the strains measured by FBG_8 and FBG_7 were much larger than those measured by other FBG sensors on the aft dome. From these results, we can find that the larger deformations occurred by the expansion in the middle of the domes and that more reinforcements in the circumferential direction of the domes are needed. In figures 7(a) and (b), the strains measured by FBG_{12}, FBG_{13}, FBG_{16}, and FBG_{17} were much larger than those measured by other FBG sensors on the cylinder and the skirt. From these results, we also find that the large deformations caused by the expansion in the middle of the cylinder can be reduced by having more reinforcements of the cylinder. Moreover, we can predict that small deformations might occur in the skirt and the skirt does not play an important role in the load bearing.

As shown in figures 6 and 7, FBG sensors bonded to the cylinder and the skirt showed close agreement with the strain gages, while there were some differences in measured strains between the FBG sensors and strain gages on the domes. The differences in strains measured by FBG sensors and strain gages may be due to a mismatch of attaching angles and locations between them. Also, this difference may be caused by the large variation of the fiber angle at points of the same meridian line in a tow prepreg of the dome as shown in figure 8. Jeusette *et al* [8] considered the variation of fiber angle along the width of the same winding tow in the analysis of a filament wound motor case. It is pointed out that the relative difference between the fiber directional strains can reach up to 40% in the polar region due to the winding angle difference along the

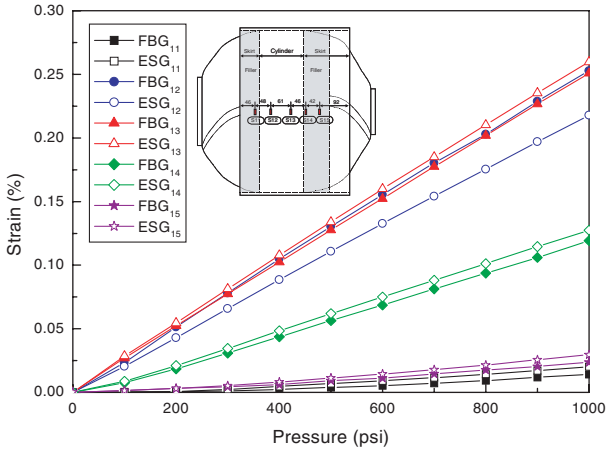

(a) Cylinder – FBG line C.

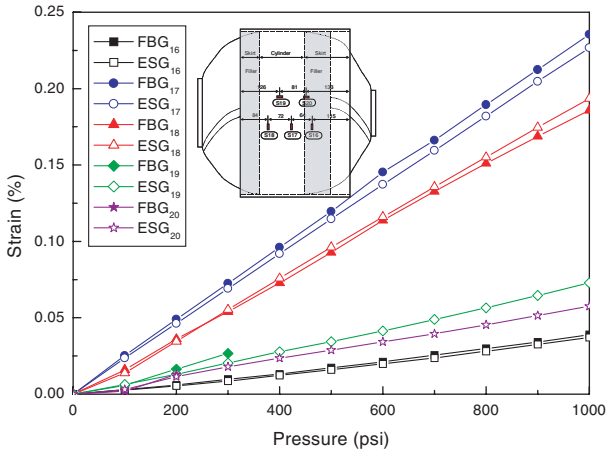

(b) Cylinder – FBG line D.

Figure 7. Strains measured by the FBG and ESG attached to the cylinder.

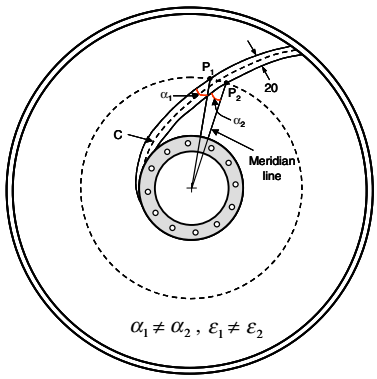

Figure 8. Angle variation along the width of the prepreg tape (P_1, P_2) on a given parallel.

width of a winding tow. In our experiment, the width of a winding tow was about 20 mm. Although each pair which consisted of a FBG sensor and a strain gage was attached at the same longitudinal location on a tow prepreg of domes, distances between FBG sensors and strain gages were about 6–8 mm. Hence, the winding angles of two points where the FBG and strain gage were attached could be different than each

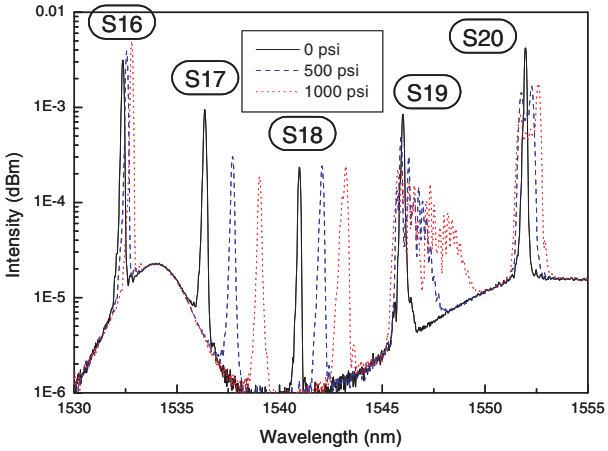

Figure 9. The variation of the FBG spectrum of FBG line D according to pressure elevation.

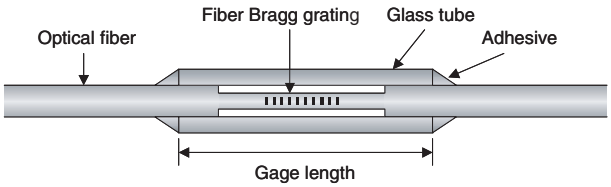

Figure 10. The configuration of the protected FBG sensor.

other. As a result, fiber directional strains measured by FBG sensors and strain gages showed remarkable discrepancies.

The signal peaks of five FBG sensors among the twenty FBG sensors split during pressurization. The peak splitting of the FBG sensor signal may occur as a result of birefringence due to transverse loading on an FBG or non-uniform strain within the grating period of an FBG. In this experiment, FBG sensors were not subjected to transverse loads. Hence, we can consider the cause of the peak splitting of the FBG signal to be the non-uniform strain within the grating period of the FBG due to a high strain gradient or a non-uniform strain distribution along the gage part of the FBG of which the length is 10 mm. Figure 9 shows the variations of FBG signal peaks of FBG line D attached to the cylinder with increasing pressure, which were acquired by an optical spectrum analyzer, using an erbium-doped fiber amplifier (EDFA) as a broadband source. FBG_{16}, FBG_{17}, FBG_{18} were attached in the hoop winding fiber direction, and FBG_{19} and FBG_{20} were affixed perpendicular to the fiber direction, i.e., in the axial direction of the cylinder, as shown in figure 5(b). Since strains in the circumferential direction of the cylinder are uniform, peaks of FBG sensor signals attached in the fiber direction did not split. However, since strains in the axial direction of the cylinder vary with a high strain gradient, the peak splitting of the signals of the FBG sensors attached in the axial direction became larger with increasing pressure. To prevent peak splitting, the FBG must be protected by an external tube such as a glass capillary tube, as shown in figure 10. By using this method, the FBG is shielded from the influences of the strain gradient and birefringence due to the transverse load. Also, the strain measured by the protected FBG is the average value of the strains applied along the gage length.

From the point of view of the measurement equipment and method, a FBG sensor system is superior to a strain gage system. Since each strain gage requires lead wires and an amplifier, increasing the number of strain gages results in a proportionally larger measurement system. Also, since the strain gage system is interfered with by electromagnetic fields, remote sensing for monitoring of hazardous structures is difficult. Conversely, since only one source is needed for numerous FBG sensors using the WDM technique, the FBG sensor system is simple. In addition, the FBG sensor system can be used for remote sensing from long distances because optical fiber is immune to electromagnetic interference. Hence, the FBG sensor system is more efficient for multiple-point strain measurements of large and hazardous structures.

5. Conclusions

20 FBG sensors were attached to the domes and cylinder parts of a filament wound composite tank to measure the strains in real time during hydrostatic pressurization. FBG sensors attached to the cylinder and the skirt showed close agreement with strain gages, while the agreement of the two types of sensor on the domes was not good. Since the signal peak splitting of some FBG sensors during pressurization makes strain measurement impossible, compensatory methods of manufacturing the sensor heads are needed to prevent the peak splitting of the FBG sensor signal. From the experiment, it was successfully demonstrated that the FBG sensor system could be useful for strain monitoring of large structures that require a large number of sensor arrays.

Acknowledgments

The authors would like to thank the Ministry of Science and Technology, Korea, for financial support by a grant from the Critical Technology 21 project.

References

[1] Kwon I B, Kim C G and Hong C S 1997 Simultaneous sensing of the strain and failure instants of composite beam using fiber optic Michelson sensor *Compos. Sci. Technol.* **57** 1639–51

[2] Foedinger R C, Rea D L, Sirkis J S, Baldwin C S, Troll J R, Grande R, Davis C S and Van Diver T L 1999 Embedded fiber optic sensor arrays for structural health monitoring of filament wound composite pressure vessels *Proc. SPIE* **3670** 289–301

[3] Kang H K, Park J W, Ryu C Y, Hong C S and Kim C G 2000 Development of fibre optic ingress/egress methods for smart composite structures *Smart Mater. Struct.* **9** 149–56

[4] Park J W, Ryu C Y, Kang H K and Hong C S 2000 Detection of buckling and crack growth in the delaminated composites using fiber optic sensor *J. Compos. Mater.* **34** 1602–23

[5] Yun S H, Richardson D J and Kim B Y 1998 Interrogation of fiber grating sensor arrays with a wavelength-swept fiber laser *Opt. Lett.* **23** 843–5

[6] Hong C S, Ryu C Y, Koo B Y, Kim C G and Yun S H 2000 Strain monitoring of smart bridge using fiber Bragg grating sensor system with wavelength-swept fiber laser *Proc. SPIE* **3988** 371–9

[7] Hong C S, Ryu C Y, Lee J R and Kim C G 2001 Bucking behavior monitoring of composite wing box model using fiber Bragg grating sensor system *Proc. SPIE* **4327** 660–8

[8] Jeusette J P, Laschet G, Charpentier P and Deloo Ph 1987 Finite element analysis of composite revolution structures wound by wide plies *Compos. Struct.* **8** 221–37